PHYSICAL REVIEW D **84,** 034028 (2011)

Phase diagrams in the hadron–Polyakov–Nambu–Jona-Lasinio model

G. Y. Shao,[1] M. Di Toro,[1,2,*] V. Greco,[1,2] M. Colonna,[1] S. Plumari,[1,2] B. Liu,[3,4] and Y. X. Liu[5,6]

[1]*INFN-Laboratori Nazionali del Sud, Via S. Sofia 62, I-95123 Catania, Italy*
[2]*Physics and Astronomy Department, University of Catania, Italy*
[3]*IHEP, Chinese Academy of Sciences, Beijing, China*
[4]*Theoretical Physics Center for Scientific Facilities, Chinese Academy of Sciences, Beijing, China*
[5]*Department of Physics and State Key Laboratory of Nuclear Physics and Technology, Peking University, Beijing 100871, China*
[6]*Center of Theoretical Nuclear Physics, National Laboratory of Heavy-Ion Accelerator, Lanzhou 730000, China*

(Received 23 May 2011; published 16 August 2011)

The two-equation of state model is used to describe the hadron-quark phase transition in dense-hot matter formed in heavy-ion collisions. The nonlinear Walecka model is used to describe the hadronic phase. For the quark phase, the Nambu–Jona-Lasinio (NJL) model coupled to Polyakov-loop fields is used to include both the chiral and (de)confinement dynamics. The phase diagrams are derived from the Gibbs conditions and compared with the results obtained in the hadron-NJL model without confinement. As in the hadron-NJL case a first order transition is observed, but with a critical end point at much higher temperatures, a consequence of the confinement mechanism that reduces the degrees of freedom of the quark matter in proximity to the phase transition. Particular attention is devoted to the phase transition in isospin asymmetric matter. Interesting isospin effects are found at high baryon density and reduced temperatures, which are in fact also common to other quark models, like the MIT bag model and the NJL model. Some possible observational signals are suggested to probe in heavy-ion collision experiments at intermediate energies.

DOI: 10.1103/PhysRevD.84.034028 PACS numbers: 12.38.Mh, 25.75.Nq

I. INTRODUCTION

The exploration of the phase diagram of strongly interacting matter and the search for the signals of the phase transition from the hadronic to the quark-gluon phase are very important in both theory and experiment. As a fundamental tool, lattice QCD provides us with the best framework for investigation of nonperturbative phenomena such as confinement and quark-gluon plasma formation at finite temperature and vanishing (small) chemical potential [1–7]. However, lattice QCD suffers from the serious problem of the fermion determinant with three colors at finite μ. Although several approximation methods have been taken to try to evade this problem [8–12], the validity of lattice simulations at finite chemical potential is still limited to the region $\mu_q/T < 1$ [13]. The results obtained with $\mu_q/T > 1$ should be taken with care.

On the other hand, many phenomenological models [14–20], as well as the more microscopic Dyson-Schwinger equations (DSEs) approach [21], have been proposed to derive a complete description of the QCD phase diagram. Among these effective models, the Nambu–Jona-Lasinio (NJL) model is a predominant one, since it offers a simple illustration of chiral-symmetry breaking and restoration, a key feature of QCD [22–28]. Moreover, it provides a complicated phase diagram of color superconductivity at high density [29–31]. One deficiency of the standard NJL model is that quarks are not confined. Recently, an improved version of the NJL model coupled to Polyakov-loop fields (PNJL) has been proposed [32]. The PNJL model takes into account both the chiral symmetry and (de)confinement effect, giving a good interpretation of lattice data at zero chemical potential and finite temperature. At the same time, it is able to make predictions in regions that cannot presently be reached in lattice calculations [19,20,33–39].

Most effective models, including the PNJL model, describe the hadron–quark-gluon phase transition based on quark degrees of freedom. As a matter of fact, at low temperatures and small chemical potential, QCD dynamics should be governed by hadrons. Therefore, it is natural to describe the strongly interacting matter with hadronic degrees of freedom at low T and small μ and quarks at high T and large μ. This picture can be easily realized following a two-equation of state (two-EoS) model, where hadronic and quark phases are connected by the Gibbs (Maxwell) criteria. Such an approach is widely used in describing the phase transition in the interior of a compact star in beta-equilibrium (e.g., [40–46]). Recently, it has also been adopted to explore the phase diagram of the hadron-quark transition at finite temperature and density related to heavy-ion collision [47–51]. Moreover, in these studies more attention was given to isospin asymmetric matter, and it was suggested that some observable effects can be seen in the charged meson yield ratio and in the onset of quark number scaling of the meson/baryon elliptic flows in Refs. [48,49]. Such a heavy-ion connection provides us

*Corresponding author.
ditoro@lns.infn.it

with a new orientation to investigate the hadron-quark phase transition, and it can stimulate some new relevant research in this field.

We have previously studied the hadron-quark phase transition in the two-EoS model by using the MIT bag model [49] and the NJL model [52], respectively, to describe quark matter. In particular, a kind of critical end point (CEP) of a first order transition has been found at about $T = 80$ MeV and $\mu = 900$ MeV when the NJL model is considered for the quark matter. In this paper, in order to obtain more reliable results and predict possible observables in the experiments, an improved calculation, within the two-EoS approach, has been performed. We take the PNJL Lagrangian to describe the properties of quark matter, with the interaction between quarks and the Polyakov loop, where both the chiral and (de)confinement dynamics are included simultaneously. We are not considering here color pairing correlations that are affecting the isospin asymmetry [51], since in heavy-ion collisions the high density system will always be formed at rather large temperatures [48].

We obtain the phase diagrams of hadron–quark-gluon phase transitions in $T - \rho_B$ and $T - \mu_B$ planes. We compare the obtained results with those given in [52], where the NJL model is used to describe the quark phase. The calculation shows that the phase-transition curves are greatly modified when both the chiral dynamics and (de)confinement effect are considered, in particular, in the high temperature and low chemical potential region. We still see a first order transition but the CEP is now at a much higher temperature and lower chemical potential. In fact, the CEP temperature is much closer to the critical temperature (for a crossover) given by the lattice calculation at vanishing chemical potential. Our results seem to stress the importance of an extension of lattice calculations up to quark chemical potentials around $\mu_q/T_c \simeq 1$.

In addition, we address the discussion about the noncoincidence of chiral and deconfinement phase transitions at large chemical potential and low temperatures, relevant to the formation of quarkyonic matter.

Finally, the calculation confirms that the onset density of the hadron-quark phase transition in isospin asymmetric matter is much smaller than that of symmetric matter, and therefore it will be more easy to probe the mixed phase in experiments.

The paper is organized as follows. In Sec. II, we describe briefly the two-EoS approach and give the relevant formulas of the hadronic nonlinear Walecka model and the PNJL effective theory. In Sec. III, we discuss the expected effects of the confinement dynamics. The quark-matter phase transition is presented in Sec. IV for the NJL as well as the PNJL model. Section V is devoted to the phase diagrams within the two-EoS frame and to the comparison with the results using only the pure quark PNJL model to describe both phases. Moreover, we present some discussions and conclusions about the phase transition, as well as some suggestions for further study. Finally, a summary is given in Sec. VI.

II. HADRON MATTER, QUARK MATTER, AND THE MIXED PHASE

In our two-EoS approach, hadron matter and quark matter are described by the nonlinear Walecka model and by the PNJL model, respectively. For the mixed phase between pure hadronic and quark matter, the two phases are connected to each other by the Gibbs conditions deduced from thermal, chemical, and mechanical equilibriums. In this section, we will first give a short introduction of the nonlinear Walecka model for hadron matter and of the PNJL model for quark matter; then we construct the mixed phase with the Gibbs criteria based on baryon and isospin charge conservations during the transition.

For the hadron phase, the nonlinear relativistic mean field (RMF) approach is used, which provides an excellent description of nuclear matter and finite nuclei as well as of compressed matter properties probed with high energy heavy-ion collisions [47–49,53,54]. The exchanged mesons include the isoscalar-scalar meson σ and isoscalar-vector meson ω (NL force, for isospin symmetric matter) and the isovector-vector meson ρ and isovector-scalar meson δ ($NL\rho$ and $NL\rho\delta$ forces, for isospin asymmetric matter).

The effective Lagrangian is written as

$$\begin{aligned}\mathcal{L} = {} & \bar{\psi}[i\gamma_\mu\partial^\mu - M + g_\sigma\sigma + g_\delta\boldsymbol{\tau}\cdot\boldsymbol{\delta} - g_\omega\gamma_\mu\omega^\mu \\ & - g_\rho\gamma_\mu\boldsymbol{\tau}\cdot\boldsymbol{\rho}^\mu]\psi + \tfrac{1}{2}(\partial_\mu\sigma\partial^\mu\sigma - m_\sigma^2\sigma^2) \\ & - \tfrac{1}{3}b(g_\sigma\sigma)^3 - \tfrac{1}{4}c(g_\sigma\sigma)^4 + \tfrac{1}{2}(\partial_\mu\delta\partial^\mu\delta - m_\delta^2\delta^2) \\ & + \tfrac{1}{2}m_\omega^2\omega_\mu\omega^\mu - \tfrac{1}{4}\omega_{\mu\nu}\omega^{\mu\nu} + \tfrac{1}{2}m_\rho^2\boldsymbol{\rho}_\mu\cdot\boldsymbol{\rho}^\mu - \tfrac{1}{4}\boldsymbol{\rho}_{\mu\nu}\cdot\boldsymbol{\rho}^{\mu\nu},\end{aligned}$$

where the antisymmetric tensors of vector mesons are given by

$$\omega_{\mu\nu} = \partial_\mu\omega_\nu - \partial_\nu\omega_\mu, \qquad \rho_{\mu\nu} \equiv \partial_\mu\rho_\nu - \partial_\nu\rho_\mu.$$

The nucleon chemical potential and effective mass in nuclear medium can be expressed as

$$\mu_i = \mu_i^* + g_\omega\omega + g_\rho\tau_{3i}\rho \tag{1}$$

and

$$M_i^* = M - g_\sigma\sigma - g_\delta\tau_{3i}\delta, \tag{2}$$

where M is the free nucleon mass, $\tau_{3p} = 1$ for the proton and $\tau_{3n} = -1$ for the neutron, and μ_i^* is the effective chemical potential which reduces to Fermi energy $E_{Fi}^* = \sqrt{k_F^{i2} + M_i^{*2}}$ at zero temperature. The baryon and isospin chemical potentials in the hadron phase are defined as

$$\mu_B^H = \frac{\mu_p + \mu_n}{2}, \qquad \mu_3^H = \frac{\mu_p - \mu_n}{2}. \tag{4}$$

The energy density and pressure of nuclear matter at finite temperature are derived as

$$\varepsilon^H = \sum_{i=p,n} \frac{2}{(2\pi)^3} \int d^3\boldsymbol{k} \sqrt{k^2 + M_i^{*2}} (f_i(k) + \bar{f}_i(k)) + \frac{1}{2} m_\sigma^2 \sigma^2 + \frac{b}{3} (g_\sigma \sigma)^3 + \frac{c}{4} (g_\sigma \sigma)^4 + \frac{1}{2} m_\delta^2 \delta^2 + \frac{1}{2} m_\omega^2 \omega^2 + \frac{1}{2} m_\rho^2 \rho^2, \tag{5}$$

$$P^H = \sum_{i=p,n} \frac{1}{3} \frac{2}{(2\pi)^3} \int d^3\boldsymbol{k} \frac{k^2}{\sqrt{k^2 + M_i^{*2}}} (f_i(k) + \bar{f}_i(k)) - \frac{1}{2} m_\sigma^2 \sigma^2 - \frac{b}{3} (g_\sigma \sigma)^3 - \frac{c}{4} (g_\sigma \sigma)^4 - \frac{1}{2} m_\delta^2 \delta^2 + \frac{1}{2} m_\omega^2 \omega^2 + \frac{1}{2} m_\rho^2 \rho^2, \tag{6}$$

where $f_i(k)$ and $\bar{f}_i(k)$ are the fermion and antifermion distribution functions for the proton and the neutron ($i = p, n$):

$$f_i(k) = \frac{1}{1 + \exp\{(E_i^*(k) - \mu_i^*)/T\}}, \tag{7}$$

$$\bar{f}_i(k) = \frac{1}{1 + \exp\{(E_i^*(k) + \mu_i^*)/T\}}. \tag{8}$$

The effective chemical potentials μ_i^* are determined by the nucleon densities

$$\rho_i = 2 \int \frac{d^3\boldsymbol{k}}{(2\pi)^3} (f_i(k) - \bar{f}_i(k)), \tag{9}$$

with the baryon number density $\rho = \rho_B^H = \rho_p + \rho_n$ and isospin density $\rho_3^H = \rho_p - \rho_n$. The asymmetry parameter can be defined as

$$\alpha^H \equiv -\frac{\rho_3^H}{\rho_B^H} = \frac{\rho_n - \rho_p}{\rho_p + \rho_n}. \tag{10}$$

In this study the parameter set $NL\rho\delta$ [48] will be used to describe the properties of hadron matter. The model parameters are determined by calibrating the properties of symmetric nuclear matter at zero temperature and normal nuclear density. Our parametrizations are also tuned to reproduce collective flows and particle production at higher energies, where some hot and dense matter is probed; see [54] and references therein.

We take the PNJL model to describe the quark matter. In the pure gauge theory, the Polyakov loop serves as an order parameter for the $\mathbb{Z}_3$ symmetry breaking transition from low to high temperatures, i.e. for the transition from a confined to a deconfined phase. In the real world quarks are coupled to the Polyakov loop, which explicitly breaks the $\mathbb{Z}_3$ symmetry. No rigorous order parameter is established for the deconfinement phase transition. However, the Polyakov loop can still be practicable to distinguish a confined phase from a deconfined one.

The Lagrangian density in the three-flavor PNJL model is taken as

$$\mathcal{L}_q = \bar{q}(i\gamma^\mu D_\mu - \hat{m}_0)q + G \sum_{k=0}^{8} [(\bar{q}\lambda_k q)^2 + (\bar{q} i\gamma_5 \lambda_k q)^2] - K[\det{}_f(\bar{q}(1+\gamma_5)q) + \det{}_f(\bar{q}(1-\gamma_5)q)] - \mathcal{U}(\Phi[A], \bar{\Phi}[A], T), \tag{11}$$

where q denotes the quark fields with three flavors, u, d, and s, and three colors, $\hat{m}_0 = \mathrm{diag}(m_u, m_d, m_s)$ in flavor space; G and K are the four-point and six-point interacting constants, respectively. The four-point interaction term in the Lagrangian keeps the $SU_V(3) \times SU_A(3) \times U_V(1) \times U_A(1)$ symmetry, while the 't Hooft six-point interaction term breaks the $U_A(1)$ symmetry.

The covariant derivative in the Lagrangian density is defined as $D_\mu = \partial_\mu - iA_\mu$. The gluon background field $A_\mu = \delta_\mu^0 A_0$ is supposed to be homogeneous and static, with $A_0 = g\mathcal{A}_0^\alpha \frac{\lambda^\alpha}{2}$, where $\frac{\lambda^\alpha}{2}$ are $SU(3)$ color generators. The effective potential $\mathcal{U}(\Phi[A], \bar{\Phi}[A], T)$ is expressed in terms of the traced Polyakov loop $\Phi = (\mathrm{Tr}_c L)/N_C$ and its conjugate $\bar{\Phi} = (\mathrm{Tr}_c L^\dagger)/N_C$. The Polyakov loop L is a matrix in color space,

$$L(\vec{x}) = \mathcal{P} \exp\left[i \int_0^\beta d\tau A_4(\vec{x}, \tau) \right], \tag{12}$$

where $\beta = 1/T$ is the inverse of the temperature and $A_4 = iA_0$.

The Polyakov loop can be expressed in a more intuitive physical form as

$$\Phi = \exp[-\beta F_q(\vec{x})], \tag{13}$$

where F_q is the free energy required to add an isolated quark to the system. So it will go from zero in the confined phase up to a finite value when deconfinement is reached [55].

In fact, the coupling to the Polyakov-loop effective field imposes a constraint only in the color space in the sense that three-quark color nonsinglets are suppressed. However, the unsuppressed color singlets are not clustered in space-time and so the hadron dynamics is not properly accounted for [56]. Since this contribution is expected to be rather important at high baryon densities and low temperatures [53], we can predict in this region large corrections to the pure PNJL results when we pass to the two-EoS picture, where an equilibrium is imposed with a hadron phase with all the baryonic interactions.

Different effective potentials are adopted in the literature [33,57,58]. The logarithmic one given in [57] will be used in our calculation, which can reproduce well the data obtained in the lattice calculation. The corresponding effective potential reads

$$\frac{\mathcal{U}(\Phi,\bar{\Phi},T)}{T^4} = -\frac{a(T)}{2}\bar{\Phi}\Phi + b(T)\ln[1 - 6\bar{\Phi}\Phi + 4(\bar{\Phi}^3 + \Phi^3) - 3(\bar{\Phi}\Phi)^2], \tag{14}$$

where

$$a(T) = a_0 + a_1\left(\frac{T_0}{T}\right) + a_2\left(\frac{T_0}{T}\right)^2 \tag{15}$$

and

$$b(T) = b_3\left(\frac{T_0}{T}\right)^3. \tag{16}$$

We note that in this version of the PNJL model the coupling between the quark condensates and the Polyakov loop is only via the covariant derivative in the Lagrangian density equation (11).

The parameters a_i, b_i are precisely fitted according to the lattice result of QCD thermodynamics in the pure gauge sector. T_0 is found to be 270 MeV as the critical temperature for the deconfinement phase transition of the gluon part at zero chemical potential [59]. When fermion fields are included, a rescaling of T_0 is usually implemented to obtain a consistent result between the model calculation and the full lattice simulation which gives a critical phase-transition temperature $T_c = 173 \pm 8$ MeV [1,2,4]. In this study we rescale $T_0 = 210$ MeV so as to produce $T_c = 171$ MeV for the phase-transition temperature at zero chemical potential.

In the mean field approximation, quarks can be seen as free quasiparticles with constituent masses M_i, and the dynamical quark masses (gap equations) are obtained as

$$M_i = m_i - 4G\phi_i + 2K\phi_j\phi_k \qquad (i \neq j \neq k), \tag{17}$$

with $i = u, d, s$, where ϕ_i stands for the quark condensate. The thermodynamic potential of the PNJL model at the mean field level is expressed as

$$\Omega = \mathcal{U}(\bar{\Phi},\Phi,T) + 2G(\phi_u^2 + \phi_d^2 + \phi_s^2) - 4K\phi_u\phi_d\phi_s - T\sum_n \int \frac{d^3p}{(2\pi)^3}\,\mathrm{Tr}\ln\frac{S_i^{-1}(i\omega_n,\vec{p})}{T}. \tag{18}$$

Here $S_i^{-1}(p) = -(\not{p} - M_i + \gamma_0(\mu_i - iA_4))$, with μ_i quark chemical potential, is the inverse fermion propagator in the background field A_4, and the trace has to be taken in color, flavor, and Dirac space. After summing over the fermion Matsubara frequencies, $p^0 = i\omega_n = (2n+1)\pi T$, the thermodynamic potential can be written as

$$\begin{aligned}\Omega = {} & \mathcal{U}(\bar{\Phi},\Phi,T) + 2G(\phi_u^2 + \phi_d^2 + \phi_s^2) - 4K\phi_u\phi_d\phi_s \\ & - 2\int_\Lambda \frac{d^3p}{(2\pi)^3}3(E_u + E_d + E_s) - 2T\sum_{u,d,s}\int\frac{d^3p}{(2\pi)^3} \\ & \times[\ln(1 + 3\Phi e^{-(E_i-\mu_i)/T} + 3\bar{\Phi}e^{-2(E_i-\mu_i)/T} \\ & + e^{-3(E_i-\mu_i)/T})] - 2T\sum_{u,d,s}\int\frac{d^3p}{(2\pi)^3}[\ln(1 + 3\bar{\Phi}e^{-(E_i+\mu_i)/T} \\ & + 3\Phi e^{-2(E_i+\mu_i)/T} + e^{-3(E_i+\mu_i)/T})],\end{aligned} \tag{19}$$

where $E_i = \sqrt{\vec{p}^2 + M_i^2}$ is the energy of quark flavor i.

We remark on some interesting differences with respect to the thermodynamical potential derived within the pure NJL model; see [27,52]. Apart from the presence of the effective potential $\mathcal{U}(\bar{\Phi},\Phi,T)$, the Polyakov loop is mostly acting on the quark-antiquark distribution functions, in the direction of a reduction on the way to confinement. This largely modifies the quark pressure, as seen in the calculations. Moreover, in spite of the minimal coupling introduced in the Lagrangian Eq. (11), only in the covariant derivative will the quark condensates be strongly affected by the Polyakov loop via the modified q, $\bar{q}$ distribution functions. This will also be clearly observed in the comparison of NJL and PNJL phase diagrams.

The values of ϕ_u, ϕ_d, ϕ_s, Φ, and $\bar{\Phi}$ are determined by minimizing the thermodynamical potential

$$\frac{\partial\Omega}{\partial\phi_u} = \frac{\partial\Omega}{\partial\phi_d} = \frac{\partial\Omega}{\partial\phi_s} = \frac{\partial\Omega}{\partial\Phi} = \frac{\partial\Omega}{\partial\bar{\Phi}} = 0. \tag{20}$$

All the thermodynamic quantities relevant to the bulk properties of quark matter can be obtained from Ω. In particular, the pressure and energy density should be zero in the vacuum.

The baryon (isospin) density and baryon (isospin) chemical potential in the quark phase are defined as follows:

$$\rho_B^Q = \tfrac{1}{3}(\rho_u + \rho_d), \qquad \rho_3^Q = \rho_u - \rho_d, \tag{21}$$

and

$$\mu_B^Q = \tfrac{3}{2}(\mu_u + \mu_d), \qquad \mu_3^Q = \tfrac{1}{2}(\mu_u - \mu_d). \tag{22}$$

The corresponding asymmetry parameter of the quark phase is defined as

$$\alpha^Q \equiv -\frac{\rho_3^Q}{\rho_B^Q} = 3\frac{\rho_d - \rho_u}{\rho_u + \rho_d}. \tag{23}$$

As an effective model, the (P)NJL model is not renormalizable, so a cutoff Λ is implemented in three-momentum space for divergent integrations. We take the model parameters $\Lambda = 603.2$ MeV, $G\Lambda^2 = 1.835$, $K\Lambda^5 = 12.36$, $m_{u,d} = 5.5$, and $m_s = 140.7$ MeV, determined by fitting f_π, M_π, m_K, and m_η to their experimental

TABLE I. Parameters in the Polyakov effective potential given in [57].

a_0	a_1	a_2	a_3
3.51	−2.47	15.2	−1.75

values [28]. The coefficients in the Polyakov effective potential are listed in Table I.

So far, we have shown how to describe the hadronic and quark phases using the RMF hadron model and the PNJL quark model, respectively. The key point in the two-EoS model is to construct the phase transition from hadronic to quark matter. As mentioned above, the two phases are connected by Gibbs criteria, i.e., the thermal, chemical, and mechanical equilibrations being required. For the hadron–quark-gluon phase transition relevant to heavy-ion collisions of duration about 10^{-22} sec (10–20 fm/c), thermal equilibration is only possible for strongly interacting processes, where baryon number and isospin conservation are preserved. So the strange-antistrange quark number may be rich, but the net strange quark number should be zero before the beginning of hadronization in the expansion stage [60], which can be approximately realized by requiring $\mu_s = 0$ (hadronization is out of the range of this study).

Based on the conservation of baryon number and isospin during strong interactions, the Gibbs conditions describing the phase transition can be expressed by

$$\begin{aligned} \mu_B^H(\rho_B, \rho_3, T) &= \mu_B^Q(\rho_B, \rho_3, T), \\ \mu_3^H(\rho_B, \rho_3, T) &= \mu_3^Q(\rho_B, \rho_3, T), \\ P^H(\rho_B, \rho_3, T) &= P^Q(\rho_B, \rho_3, T), \end{aligned} \tag{24}$$

where

$$\begin{aligned} \rho_B &\equiv \rho_B(\chi) = (1-\chi)\rho_B^H + \chi\rho_B^Q, \\ \rho_3 &\equiv \rho_3(\chi) = (1-\chi)\rho_3^H + \chi\rho_3^Q \end{aligned} \tag{25}$$

are the total baryon density and isospin density inside the mixed phase, respectively, and χ is the fraction of quark matter.

The global asymmetry parameter α in the mixed phase is

$$\alpha \equiv -\frac{\rho_3(\chi)}{\rho_B(\chi)} = -\frac{(1-\chi)\rho_3^H + \chi\rho_3^Q}{(1-\chi)\rho_B^H + \chi\rho_B^Q} \tag{26}$$

which is a constant determined by the heavy-ion source formed in experiments. With the definition of α given above, α^H for the pure hadron phase and α^Q for the pure quark phase can be obtained with $\chi = 0$ and 1, respectively. This is evident by comparing Eqs. (10) and (23) with Eq. (26). Although α^H for the pure hadronic phase ($\chi = 0$) and α^Q for the pure quark phase ($\chi = 1$), as well as α for the mixed phase, remain constant for a given reaction (e.g., a ^{238}U + ^{238}U collision) in experiments, the asymmetry parameters α^H, α^Q inside the mixed phase with $0 < \chi < 1$ can vary with the quark concentration χ; see also the discussion after Fig. 7 in Sec. V.

III. EXPECTED EFFECT OF THE CONFINEMENT DYNAMICS

Before showing detailed phase diagram results within the two-EoS approach, it is very instructive to analyze the effects of chiral and (de)confinement dynamics in the pure quark sector. In order to understand the physics behind this, we will show separately the results in the NJL, with the same parameters given before, and the PNJL model, for isospin symmetric matter. In Figs. 1 and 2 we plot the pressure of isospin symmetric quark matter as a function of

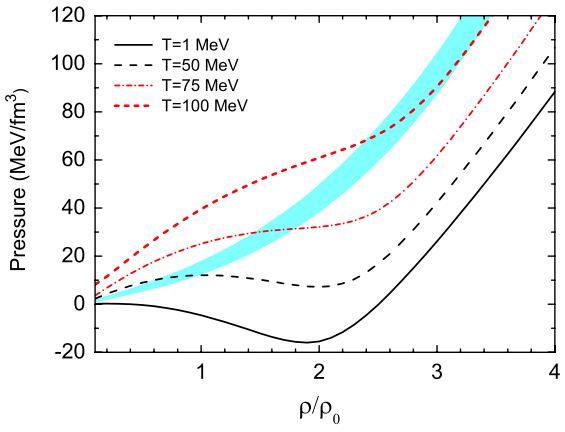

FIG. 1 (color online). Pressure of quark matter as a function of baryon density at different temperatures in the NJL model. We show the case of isospin symmetric matter. In the shaded area we show also the hadron (NL) curves in the temperature region between 50 and 75 MeV.

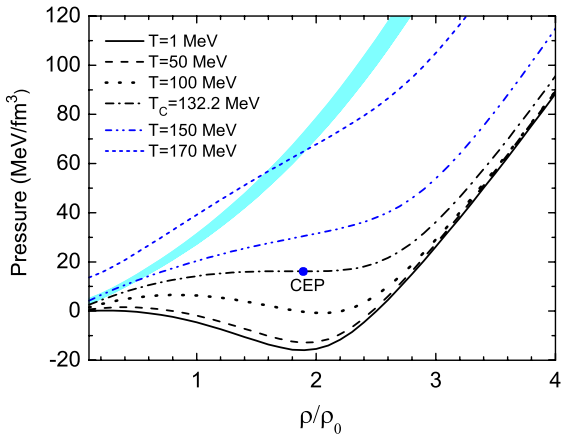

FIG. 2 (color online). Pressure of quark matter as a function of baryon density at different temperatures in the PNJL model. We show the case of isospin symmetric matter. In the shaded area we show also the hadron (NL) curves in the temperature region between 150 and 170 MeV.

baryon density for different temperatures, respectively, for the NJL and PNJL models. In this calculation isospin symmetric matter with $\mu = \mu_u = \mu_d$ and $\mu_s = 0$ is considered, and ϕ_l stands for the chiral condensate of u, d quarks.

The contribution of the pion gas to the hadronic pressure has not been included in the present calculation. For isospin symmetric matter, with zero π-chemical potential [47], this part is rather small at the finite temperatures of interest here; see also [53]. For asymmetric neutron-rich matter, a π^- condensate may appear for very isospin asymmetric matter with $\mu_p - \mu_n = -m_\pi$ [47]. Such larger isospin asymmetry appears well beyond the experimentally accessible region in heavy-ion collisions, and so the π condensate is also not considered in the present calculation.

From the two figures, we can see that the pressure has a local maximum and a local minimum at low temperatures. The local extrema will disappear with the increase of temperature. The temperature with the disappearance of the two local extrema corresponds to the CEP of the first order chiral transition; for a more detailed discussion please refer to [27,34]. It is interesting to note that the critical temperature of the chiral transition is rather different in the two cases, around 70 MeV in the NJL model and around 130 MeV in the PNJL model, while the density region of the mixed phase is not affected much. This is due to the fact that for a fixed baryon density (or chemical potential) the NJL model presents a much larger pressure for a given temperature, as clearly seen from Figs. 1 and 2 [61]. This is a nice indication that when we have a coupling to the confinement, even in the minimal way included here, the quark pressure at finite temperatures is reduced since the quark degrees of freedom start to decrease.

All that will imply important differences at higher temperatures since above the chiral restoration the quark pressure will rapidly increase, reaching an end point in the two-EoS approach where the matching to the hadron pressure will not be possible. This will happen at different points of the (T, μ), (T, ρ) planes for the hadron-NJL [52] and the hadron-PNJL models, and higher temperatures will be requested in the PNJL case. In fact, this can also be clearly seen from Figs. 1 and 2, of the NJL and PNJL pressures, where we also plot the corresponding curves of the hadronic EoS in the end-point regions (shaded area). The Gibbs (Maxwell) conditions have no solution with decreasing density (chemical potential) and increasing temperature if we encounter a crossing of the hadron and quark curves in the $T - \rho_B$ $(T - \mu_B)$ plane, with the quark pressure becoming larger than the hadron one. We see that this happens for $T \simeq 75$ MeV and $\rho/\rho_0 \simeq 1.8$ in the NJL case and for $T \simeq 170$ MeV and $\rho/\rho_0 \simeq 1.6$ in the PNJL quark picture.

Of course a similar effect on the variation of the CEP can be obtained by inserting a phenomenological bag pressure parameter $B(T, \mu_B)$, which is temperature and chemical potential dependent, in the quark EoS. The point is that this will not have any consistent physics foundation, while the relation between the CEP and chiral dynamics in the NJL scheme is very clear [52], as is the further contribution of the confinement dynamics described here.

In conclusion, due to the noticeable quark pressure difference at finite temperatures, besides the critical end points, we expect, in general, rather different phase diagrams given by the hadron-NJL and hadron-PNJL models. This will be seen in Sec. V, Figs. 8 and 9.

IV. PNJL PHASE DIAGRAM IN THE QUARK SECTOR

In order to better understand the effects of the coupling between quark condensates and the Polyakov loop and also to compare with the two-EoS results, we also discuss here the phase diagram in the pure quark sector obtained from the PNJL model.

We plot in Fig. 3 the temperature evolution of the chiral condensate ϕ_l and the Polyakov loop Φ for various values of the quark chemical potential. Φ and $\bar{\Phi}$ have the same values at zero chemical potential, and their difference is very small at finite chemical potential; hence, we only present the results of Φ in Fig. 3 and later in the discussion.

First, we can see that the chiral condensate and Polyakov loop Φ vary continuously at $\mu = 0$ and 200 MeV, and there exist sharp decreases (increases) at high temperatures indicating the onset of chiral (deconfinement) phase transitions. These characteristics show that the corresponding chiral and deconfinement phase transitions are crossovers for small chemical potential at high temperatures. At variance, for large chemical potentials, e.g., $\mu = 350$ MeV, the chiral condensate varies discontinuously with the temperature, which indicates the presence of a first order chiral phase transition, as already seen in the pure NJL approach,

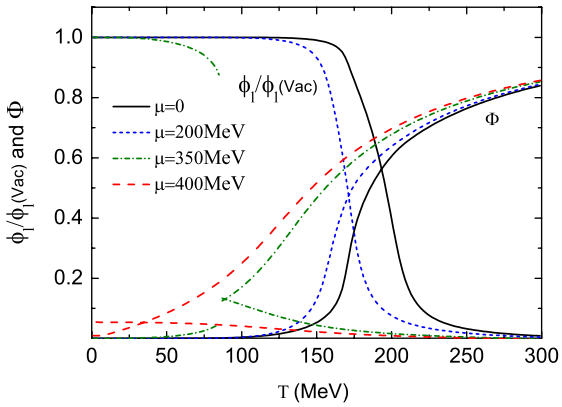

FIG. 3 (color online). Chiral condensate ϕ_l (normalized to the vacuum value) and Polyakov loop Φ as functions of temperature for various values of the quark chemical potential. We show the case of isospin symmetric matter.

although at much lower temperatures [27], as discussed in the previous section. The Polyakov loop always shows a continuous behavior, indicating that we have only crossover transitions. The jump observed for the dash-dotted curve corresponding to a $\mu = 350$ MeV chemical potential is just an effect of the coupling to the sharp variation of the quark condensates at the first order chiral transition. Moreover, this happens in a region of very small values of the Φ field at lower temperatures. As a matter of fact, such a discontinuity disappears for the results at $\mu = 400$ MeV, i.e. above the chiral transition; see the dashed curves for both the ϕ and Φ fields.

Finally, in Fig. 4 we plot the phase diagram of the PNJL model in the $T - \mu_q$ plane (always for isospin symmetric matter). The phase-transition curves are obtained by requiring that $\partial\phi_l/\partial T$ and $\partial\Phi/\partial T$ take the maximum values. For the deconfinement phase transition the use of the maximum value of $\partial\Phi/\partial T$ as the phase-transition tracer is a good choice when μ is not too large. In fact, we see from Fig. 3 a sharp increase of Φ for $\mu = 0$ and 200 MeV. However, with the increase of chemical potential, although we are still able to observe the maximum of $\partial\Phi/\partial T$, the width of the maximum increases. The peaks of $\partial\Phi/\partial T$ are more smoothed and the maximum value will not be a well-defined phase transition tracer anymore as μ is large. Therefore, some authors take $\Phi = 1/2$ as the phase-transition parameter [58,62,63]. In conclusion, from Fig. 3 we can see that the chiral phase transition is continuous at high temperatures and relatively smaller chemical potential, while a first order phase transition takes place at low temperatures and larger chemical potential. The CEP of the chiral transition appears at (132.2, 296.6) MeV in the $T - \mu_q$ plane, in agreement with similar calculations [63]. At variance, the deconfinement phase transition is always a continuous crossover in the PNJL model, but the peak of $\partial\Phi/\partial T$ becomes more and more smooth with the increase of baryon chemical potential.

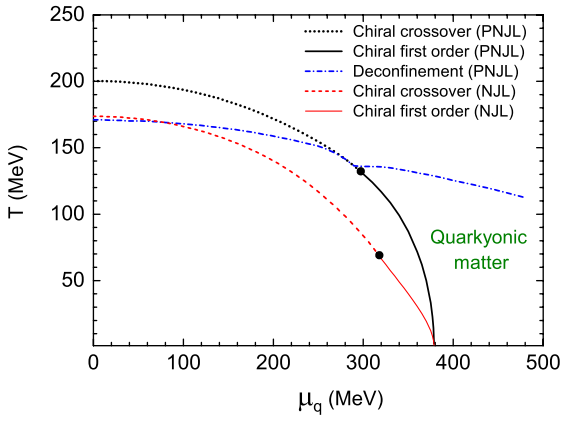

FIG. 4 (color online). Phase diagram of the PNJL model. The corresponding chiral phase transition for the pure NJL model is also shown. We show the case of isospin symmetric matter.

In addition, at large chemical potential, chirally restored but still confined matter, the hypothetical quarkyonic matter suggested by McLarren and Pisarski [64], can be realized in the PNJL model. We remind the reader again that the confinement here means only the three-quark color singlet correlation, without any space-time clustering. The interaction between these three-quark color correlated compounds is then different from the baryon interaction (with chiral restored constituent quarks) [56]. All this is reported in Fig. 4, where we plot the full phase diagram of the PNJL approach.

Here we give a short discussion about the coincidence of chiral and deconfinement phase transitions, as well as the presence of quarkyonic matter. The temperature dependence of the chiral condensate and of the Polyakov loop of Fig. 3, as well the PNJL phase diagram of Fig. 4, are obtained with the rescaled parameter $T_0 = 210$ MeV. The coincidence of chiral restoration and deconfinement takes place at about $\mu_q = 290$ MeV. If we take $T_0 = 270$ MeV, the approximate coincidence, with the different phase-transition temperatures less than 10 MeV, will move down to $\mu \simeq 0$. In any case, there is only one crossing point of the two phase transitions. Up to now, the relation between chiral-symmetry restoration and the deconfinement phase transition is still an open question. It is possible that the coincidence of chiral and deconfinement phase transitions takes place in a wider range of chemical potentials. Such coincidence has indeed been realized recently by considering a larger coupling (entanglement) between the chiral condensate and Polyakov loop with a chemical potential dependent T_0 and/or an explicit Φ dependence of the condensate coupling $G(\Phi)$ [62,63].

Also in Fig. 4, we report the chiral transition curve for the pure NJL model (same parameters). We note the coupling between the chiral condensates and the Polyakov-loop fields $(\Phi, \bar{\Phi})$ mostly affects the temperature of the chiral CEP as expected from the pressure discussion of the previous section.

From Fig. 4 we can see that the deconfinement phase-transition temperature is still high at large chemical potential, and so the region of quarkyonic matter appears very wide. On the other hand, the signature of a deconfinement transition disappears at large chemical potentials and lower temperatures. Because of the lack of lattice-QCD data at large real chemical potentials, more investigations are needed to study the physics in this range. The results in [62] also show that the range of quarkyonic matter shrinks when a μ-dependent T_0 and/or a larger entanglement between the quark condensate and Polyakov loop is considered.

We remark that this $(T - \mu)$ zone just represents the nuclear matter phase diagram region possibly reached in the collision of heavy ions at intermediate energies. Therefore, it is of large interest to perform two-EoS predictions with a good connection to the more fundamental

results of effective quark models. This is the subject of the next section.

V. HADRON-QUARK PHASE TRANSITIONS

In the following we will discuss the phase diagrams obtained in the two-EoS model, i.e., explicitly considering a hadronic EoS with the parameter set NL for symmetric matter and $NL\rho\delta$ for asymmetric matter at low density and chemical potential [48,65].

We present first the phase transition from the hadronic to the deconfined quark phase in the $T-\rho_B$ plane in Fig. 5 for symmetric matter and in Fig. 6 for asymmetric matter with the global asymmetry parameter $\alpha = 0.2$. For symmetric matter at a fixed T, the first order phase transition takes place with the same pressure and μ_B in both phases, but a jump of ρ_B^H to ρ_B^Q, just as shown in Fig. 5. In the mixed phase, the pressures of both phases remain unchanged and $\alpha = \alpha^H = \alpha^Q = 0$ for any quark fraction χ. These features are quite different for the mixed phase in isospin asymmetric matter. As already noted in [52], where the NJL quark EoS has been used, also in the PNJL case we see a clear isospin distillation effect, i.e., a strong enhancement of the isospin asymmetry in the quark component inside the mixed phase, as reported in Fig. 7, where the asymmetry parameters in the two components are plotted vs the quark fraction χ. As a consequence, the pressure in the mixed phase keeps rising with χ, more rapidly for quark concentrations below 50% [52].

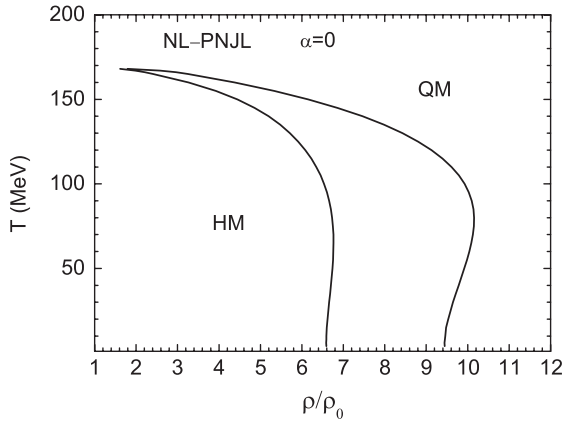

FIG. 5. Phase diagram in the $T-\rho_B$ plane in the two-EoS model for symmetric matter.

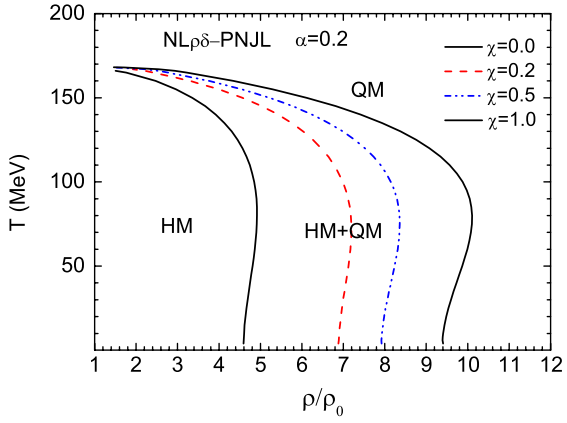

FIG. 6 (color online). Phase diagram in the $T-\rho_B$ plane in the two-EoS model for asymmetric matter with the global asymmetry parameter $\alpha = 0.2$. χ represents the fraction of quark matter.

From Fig. 7 we remark that this isospin enrichment of the quark phase is rather robust vs the increasing temperature. This is important since color pairing correlations at low temperatures will decrease symmetry energy effects [51]. We have to note that such large isospin distillation effects are due to the large difference in the symmetry terms in the two phases, mainly because all the used quark effective models do not have explicit interaction isovector fields [49].

Such behavior of the local asymmetry parameters will possibly produce some observational signals in the following hadronization during the expansion. We can expect an inverse trend in the emission of neutron-rich clusters, as well as an enhancement of π^-/π^+, K^0/K^+ yield ratios from the high density n-rich regions which undergo the transition. Besides, an enhancement of the production of isospin-rich resonances and subsequent decays may be found. For more details one can refer to [49,52].

An evident feature of Fig. 6 is that at lower temperatures the onset density of the hadron-quark phase transition for asymmetric matter is much lower than that of the symmetric one, and therefore it will be easier to probe in heavy-ion collision experiments. At variance, the CEP, at $T \simeq 170$ MeV and $\rho/\rho_0 \simeq 1.6$, appears almost unaffected by the isospin asymmetry of matter, as we see by comparing Figs. 5 and 6. The reason is that the hadronic symmetry energy is largely reduced at very high temperatures for the large smoothing of the fermion distributions, in the kinetic

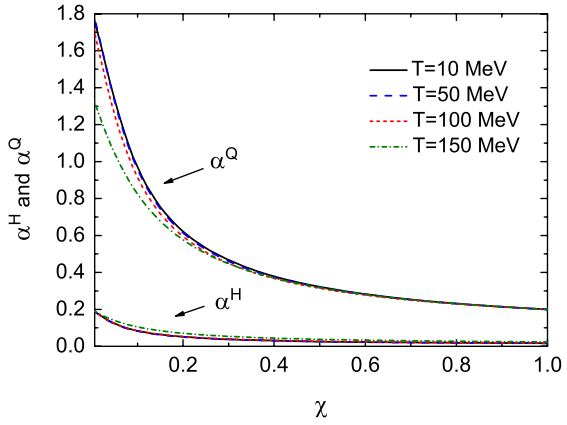

FIG. 7 (color online). The behavior of local asymmetric parameters α^H and α^Q in the mixed phase for several different temperatures. The parameter set $NL\rho\delta$ is used in the calculation.

as well as in the interaction contributions. This effect is in fact present in all the other hadron-quark two-EoS models [49,52,53].

We plot the $T - \mu_B$ phase diagrams in Fig. 8 for symmetric matter and in Fig. 9 for asymmetric matter. Figure 8 clearly shows that there is only one phase-transition curve in the $T - \mu_B$ plane. The phase-transition curve is independent of the quark fraction χ. However, for asymmetric matter, the phase-transition curve varies for different quark fractions χ. The phase-transition curves in Fig. 9 are obtained with $\chi = 0$ and 1, representing the beginning and the end of the hadron-quark phase transition, respectively.

In Figs. 8 and 9 we also plot the phase-transition curves with the hadron-NJL model. For the NJL model with only chiral dynamics, no physical solution exists when the temperature is higher than ~80 MeV. The corresponding temperature is enhanced to about ~166 MeV with the hadron-PNJL model, which is closer to the phase transition (crossover) temperature given by the full lattice calculation

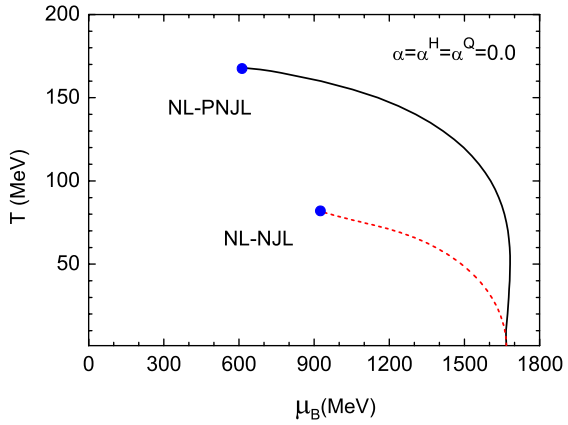

FIG. 8 (color online). Phase diagram in the $T - \mu_B$ plane for symmetric matter.

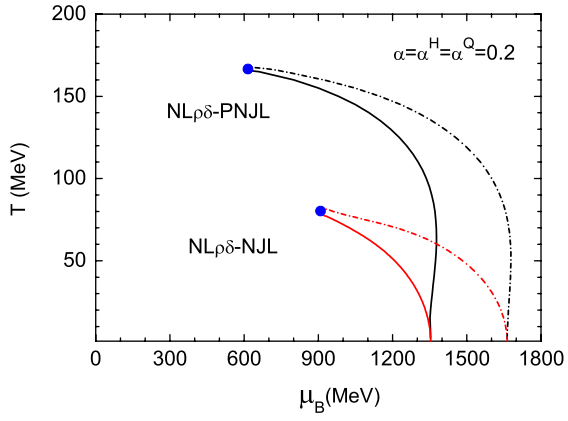

FIG. 9 (color online). Phase diagram in the $T - \mu_B$ plane for asymmetric matter with the global asymmetry parameter $\alpha = 0.2$.

at zero or small chemical potential [1,2,4]. In this sense the hadron-PNJL model gives significantly different results and certainly represents an improvement with respect to the hadron-NJL model of Ref. [52]. From Fig. 9 we remark that in both cases the region around the critical end points is almost unaffected by isospin asymmetry contributions, which are relevant at lower temperatures and larger chemical potentials.

From the detailed discussions of the previous two sections we now nicely understand the large difference between hadron-NJL and hadron-PNJL phase transitions and the important role of the confinement dynamics.

Finally, in Fig. 10 we present, together, the phase diagrams obtained with the PNJL model and the hadron-PNJL model. We find that the deconfined phase-transition curve in the PNJL model is close to that obtained in the hadron-PNJL model at high temperatures and intermediate chemical potential. At larger chemical potential, the deconfinement phase-transition curve in the PNJL model still has a high temperature. On the other hand, in the previous section we have seen that the deconfinement phase-transition order parameter Φ cannot describe well the phase transition at larger chemical potential and lower temperatures. We must rely on the predictions of the two-EoS approach, which in fact nicely show a good connection to the results more reliable in the PNJL quark model, at high temperatures and small or vanishing chemical potential. The two-EoS hadron-(P)NJL model also shows that the phase transition at low temperatures takes place at much larger chemical potential, consistent with the expectation of a more relevant contribution from the hadron sector [53].

From Fig. 10 we also see that at temperatures below 100 MeV there is room for the existence of the hypothetical quarkyonic matter, in the PNJL sense, i.e. in any case not a pure baryonic matter, since the chemical potential of the deconfinement transition is well above the chiral restoration line for the quark matter. However, this cannot be definitively stated until we are unable to get a unique EoS

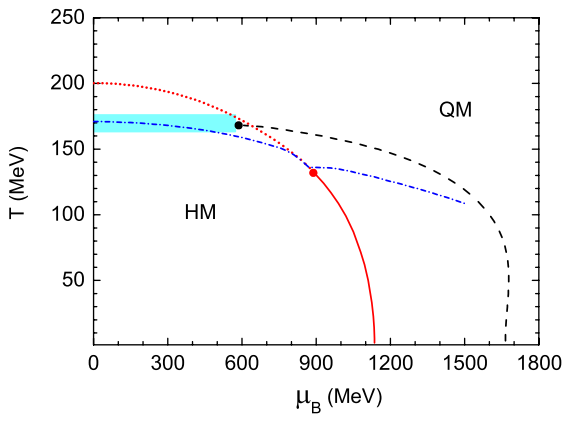

FIG. 10 (color online). Phase diagram of the PNJL model and the two-EoS model (dashed curve). The shaded area is just a guide for the eye.

that can describe all phases, hadronic as well as quark chiral restored and deconfined.

We notice that at $T = 0$ there is no difference between the hadron-NJL and hadron-PNJL models. This is due to the fact that there is no dependence of Φ on μ_B; therefore, it vanishes and the PNJL model reduces to the NJL model. This may cast some doubt on the reliability of the present calculations at $T = 0$ and large μ_B. However, our main interest is in the $T \simeq 50$–100 MeV region that can be reached by heavy-ion collisions at relativistic energies.

It interesting to remark that our two-EoS phase diagram of Fig. 10 is very similar to the results obtained in [19]; see Fig. 3 of that work, where a hadronic model has been phenomenologically extended to include quark degrees of freedom, with chiral and confinement dynamics. An extension of the Polyakov-loop Φ potential has been used, even dependent on the chemical potential, which allows us to better account for deconfinement at higher baryon densities. It seems that one- and two-EoS models nicely give similar results if the same physics effects are included, a good perspective for the future and also for possible experimental suggestions.

Moreover, the results obtained by the hadron-PNJL model at high T, small μ_B and at low T, large μ_B may be improved with the consideration of a stronger entanglement between the chiral condensate and Polyakov loop and/or a chemical potential dependent T_0. The relevant investigation will be performed as a further study. In any case, since we lack reliable lattice data at large chemical potential, more theoretical work, in general, is encouraged.

VI. SUMMARY

In this study, the hadron-quark phase transitions are investigated in the two-EoS model. The nonlinear Walecka model and the PNJL (NJL) model are used to describe hadron matter and quark matter, separately. We follow the Gibbs criteria to construct the mixed phase with baryon number and isospin conservations, likely reached during the hot and dense phase formed in heavy-ion collisions at intermediate energies. The parameters in both models are well fitted to give a good description of the properties of nuclear matter (even isospin asymmetric), at saturation as well as at higher baryon densities, or lattice data at high temperatures with zero/small chemical potential.

The main problem of the two-EoS scheme is that the Gibbs equations to link the two phases give only the conditions to have the hadron/quark system in equilibrium with the same intensive thermodynamical variables, temperature, pressure, and chemical potentials. We can interpret it as the possibility for a first order phase transition, but we do not have access to other important information, like discontinuities of order parameters and/or the detailed space-time structure of the mixed phase. In order to get all that, it is essential to have both phases described by the same EoS, as we have nicely seen for the low energy liquid-gas transition of nucleonic matter [65]. Unfortunately, this is not presently available, but properties of the coexistence zone can already supply valuable predictions. In this sense it is also nice to have cross-checks with other one-EoS effective QCD models with similar physics content, like Ref. [19].

The phase diagrams for both symmetric and asymmetric matter are explored in both the $T - \rho_B$ and $T - \mu_B$ planes. In both hadron-(P)NJL calculations we get a first order phase transition with a critical end point at finite temperature and chemical potential. In the PNJL case the CEP is shifted to larger temperatures and a smaller chemical potential, to the (166 600) MeV point in the (T, μ_B) plane. This appears to be a nice indication of a decrease of the quark pressure when confinement is accounted for. Such a result is particularly interesting since the CEP is now in the region of $\mu_q/T_c \simeq 1$ (where μ_q is the quark chemical potential), so it could be reached with some confidence by lattice-QCD complete calculations.

Another interesting result is that isospin effects are almost negligible when we approach the CEP. At variance, the calculation shows that the onset density of asymmetric matter is lower than that of symmetric matter. Moreover, in the mixed phase of asymmetric matter, the decrease of the local asymmetry parameters α^H and α^Q with the increase of the quark fraction χ may produce some observable signals. In particular, we remark that there is a noticeable isospin distillation mechanism (isospin enrichment of the quark phase) at the beginning of the mixed phase, i.e. for low quark fractions, that should show up in the hadronization stage during the expansion. We also see from Fig. 7 that this effect is still there even at relatively large temperatures, certainly present in the high density stage of heavy-ion collisions at relativistic energies [48,54]. All this supports the possibility of an experimental observation in the new planned facilities, for example, FAIR at GSI-Darmstadt and NICA at JINR-Dubna, with realistic asymmetries for stable/unstable beams. Some expected possible signals are suggested.

Because of the lack of lattice data at larger, real chemical potentials, we are left with the puzzle between chiral-symmetry restoration and deconfinement. More investigations on the chiral dynamics and (de)confinement, as well as their entanglement, are needed. The improvement of the understanding of the quark-matter interaction is beneficial to get more accurate results in the two-EoS model.

ACKNOWLEDGMENTS

This project has been supported in part by the National Natural Science Foundation of China under Grants No. 10875160, No. 11075037, and No. 10935001, and by the Major State Basic Research Development Program under Contract No. G2007CB815000. This work has been partially performed under the FIRB Research Grant RBFR0814TT provided by the MIUR.

[1] F. Karsch, E. Laermann, and A. Peikert, Nucl. Phys. **B605**, 579 (2001).
[2] F. Karsch, Nucl. Phys. **A698**, 199 (2002).
[3] C. R. Allton *et al.*, Phys. Rev. D **66**, 074507 (2002).
[4] M. Kaczmarek and F. Zantow, Phys. Rev. D **71**, 114510 (2005).
[5] M. Cheng *et al.*, Phys. Rev. D **74**, 054507 (2006).
[6] Y. Aoki *et al.*, J. High Energy Phys. 06 (2009) 088.
[7] S. Borsányi *et al.*, J. High Energy Phys. 09 (2010) 073.
[8] Z. Fodor and S. D. Katz, Phys. Lett. B **534**, 87 (2002); J. High Energy Phys. 03 (2002) 014.
[9] Z. Fodor, S. D. Katz, and C. Schmidt, J. High Energy Phys. 03 (2007) 121.
[10] M. D'Elia and F. Sanfilippo, Phys. Rev. D **80**, 014502 (2009).
[11] S. Ejiri, Phys. Rev. D **78**, 074507 (2008).
[12] M. A. Clark and A. D. Kennedy, Phys. Rev. Lett. **98**, 051601 (2007).
[13] K. Fukushima and T. Hatsuda, Rep. Prog. Phys. **74**, 014001 (2011).
[14] Y. Nambu and G. Jona-Lasinio, Phys. Rev. **122**, 345 (1961); **124**, 246 (1961).
[15] D. Toublan and J. B. Kogut, Phys. Lett. B **564**, 212 (2003).
[16] S. B. Rüster, V. Werth, M. Buballa, I. A. Shovkovy, and D. H. Rischke, Phys. Rev. D **72**, 034004 (2005).
[17] D. Blaschke *et al.*, Phys. Rev. D **72**, 065020 (2005).
[18] H. Abuki and T. Kunihiro, Nucl. Phys. **A768**, 118 (2006).
[19] V. A. Dexheimer and S. Schramm, Phys. Rev. C **81**, 045201 (2010).
[20] J. Steinheimer, V. A. Dexheimer, H. Petersen, M. Bleicher, S. Schramm, and H. Stöcker, Phys. Rev. C **81**, 044913 (2010).
[21] Si-xue Qin, Lei Chang, Huan Chen, Yu-xin Liu, and Craig D. Roberts, Phys. Rev. Lett. **106**, 172301 (2011).
[22] M. K. Volkov, Ann. Phys. (N.Y.) **157**, 282 (1984).
[23] T. Hatsuda and T. Kunihiro, Phys. Lett. **145B**, 7 (1984).
[24] S. P. Klevansky, Rev. Mod. Phys. **64**, 649 (1992).
[25] T. Hatsuda and T. Kunihiro, Phys. Rep. **247**, 221 (1994).
[26] R. Alkofer, H. Reinhardt, and H. Weigel, Phys. Rep. **265**, 139 (1996).
[27] M. Buballa, Phys. Rep. **407**, 205 (2005).
[28] P. Rehberg, S. P. Klevansky, and J. Hüfner, Phys. Rev. C **53**, 410 (1996).
[29] I. Shovkovy and Mei Huang, Nucl. Phys. **B564**, 205 (2003).
[30] M. Huang and I. Shovkovy, Nucl. Phys. **A729**, 835 (2003).
[31] M. Alford, A. Schmit, K. Rajagopal, and T. Schäfer, Rev. Mod. Phys. **80**, 1455 (2008), and references therein.
[32] K. Fukushima, Phys. Lett. B **591**, 277 (2004).
[33] C. Ratti, M. A. Thaler, and W. Weise, Phys. Rev. D **73**, 014019 (2006).
[34] P. Costa, M. C. Ruivo, C. A. de Sousa, and H. Hansen, SIGMA **2**, 1338 (2010).
[35] B-J. Schaefer, M. Wagner, and J. Wambach, Phys. Rev. D **81**, 074013 (2010).
[36] T. K. Herbst, J. M. Pawlowski, and B-J. Schaefer, Phys. Lett. B **696**, 58 (2011)
[37] K. Kashiwa, H. Kouno, M. Matsuzaki, and M. Yahiro, Nucl. Phys. **B662**, 26 (2008).
[38] H. Abuki, R. Anglani, R. Gatto, G. Nardulli, and M. Ruggieri, Phys. Rev. D **78**, 034034 (2008).
[39] W. J. Fu, Z. Zhang, and Y. X. Liu, Phys. Rev. D **77**, 014006 (2008).
[40] N. K. Glendenning, Phys. Rev. D **46**, 1274 (1992).
[41] N. K. Glendenning and J. Schaffner-Bielich, Phys. Rev. Lett. **81**, 4564 (1998); Phys. Rev. C **60**, 025803 (1999).
[42] G. F. Burgio, M. Baldo, P. K. Sahu, and H.-J. Schulze, Phys. Rev. C **66**, 025802 (2002).
[43] T. Maruyama, S. Chiba, H-J. Schulze, and T. Tatsumi, Phys. Rev. D **76**, 123015 (2007).
[44] F. Yang and H. Shen, Phys. Rev. C **77**, 025801 (2008).
[45] G. Y. Shao and Y. X. Liu, Phys. Rev. C **82**, 055801 (2010).
[46] J. Xu, L. W. Chen, C. M. Ko, and B. A. Li, Phys. Rev. C **81**, 055803 (2010).
[47] H. Müller, Nucl. Phys. **A618**, 349 (1997).
[48] M. Di Toro, A. Drago, T. Gaitanos, V. Greco, and A. Lavagno, Nucl. Phys. **A775**, 102 (2006).
[49] M. Di Toro *et al.*, Phys. Rev. C **83**, 014911 (2011).
[50] R. Cavagnoli, C. Providência, and D. P. Menezes, Phys. Rev. C **83**, 045201 (2011).
[51] G. Pagliara and J. Schaffner-Bielich, Phys. Rev. D **81**, 094024 (2010).
[52] G. Y. Shao, M. Di Toro, B. Liu, M. Colonna, V. Greco, Y. X. Liu, and S. Plumari, Phys. Rev. D **83**, 094033 (2011).
[53] B. Liu, M. Di Toro, G. Y. Shao, V. Greco, C. W. Shen, and Z. H. Li, arXiv:1105.0555.
[54] M. Di Toro *et al.*, Prog. Part. Nucl. Phys. **62**, 389 (2009).
[55] L. D. McLarren and B. Svetitski, Phys. Rev. D **24**, 450 (1981).
[56] W. Weise, arXiv:1009.6210.
[57] S. Rößner, C. Ratti, and W. Weise, Phys. Rev. D **75**, 034007 (2007).
[58] K. Fukushima, Phys. Rev. D **77**, 114028 (2008).
[59] M. Fukugita, M. Okawa, and A. Ukava, Nucl. Phys. **B337**, 181 (1990).
[60] C. Greiner, P. Koch, and H. Stoecker, Phys. Rev. Lett. **58**, 1825 (1987).
[61] H. Hansen, W. M. Alberico, A. Beraudo, A. Molinari, M. Nardi, and C. Ratti, Phys. Rev. D **75**, 065004 (2007).
[62] Y. Sakai, T. Sasaki, H. Kouno, and M. Yahiro, arXiv:1104.2394v1 [Phys. Rev. D (to be published)].
[63] Y. Sakai, T. Sasaki, H. Kouno, and M. Yahiro, Phys. Rev. D **82**, 076003 (2010).
[64] L. McLarren and R. D. Pisarski, Nucl. Phys. **A796**, 83 (2007); Y. Hidaka, L. McLarren, and R. D. Pisarski, Nucl. Phys. **A808**, 117 (2008).
[65] V. Baran, M. Colonna, V. Greco, and M. Di Toro, Phys. Rep. **410**, 335 (2005).